NON-ISOTHERMAL MODELING OF DRYING KINETICS OF CERAMIC TILES

Juan Carlos Jarque[1], Carmen Segarra[1], Vicente Cantavella[1], Rosa Mondragón[2*]

[1] Instituto de Tecnología Cerámica. Universitat Jaume I.

Campus de Riu Sec. 12071-Castellón de la Plana. Spain

[2] Departamento de Ingeniería Mecánica y Construcción. Universitat Jaume I

Campus de Riu Sec. 12071-Castellón de la Plana. Spain

* Corresponding author. E-mail: mondragn@uji.es. Tel: +34 964728146. Fax: +34 964728106

Abstract

The present study has been undertaken to optimise the drying stage in ceramic tile manufacture. Tests were conducted to determine drying kinetics, establishing how air temperature and relative humidity influenced this process. Tests show that surface moisture content does not evolve as might be expected on the basis of the simple assumption that the surface dries immediately and reaches equilibrium moisture content. A non-isothermal model was proposed to model drying curves successfully. The influence of drying temperature, bulk density of the shaped material and tile thickness on the drying process and the parameters of the model was obtained.

Key words: Drying, kinetics, mass transfer, ceramic tiles, microstructure

1 Introduction

The basic drying operation has been widely studied. However, studies have largely focused on identifying the material properties that most affect drying kinetics, and on analysing how those properties vary with the temperature, moisture and microstructure of the solid. These studies allow a comparative analysis of the materials but the results are not readily extrapolable to industrial conditions. The knowledge of the evolution of moisture content during drying is necessary for good control of quality product and to optimize the drying conditions and the dryer selection.

In general, drying processes can be divided into two drying stages (1, 2). During the first drying period the shaped solid enters the hot medium, undergoes sensible heating up to wet bulb temperature and then evaporation from the surface starts. The moisture migrates from the inner part of the solid, rapidly enough to maintain surface saturation. This stage is also known as the constant rate period, since the change of moisture per unit time remains steady. At the critical moisture content, the surface cannot longer be maintained saturated by moisture migration and the second drying period begins. In this period, called falling rate period, the evaporation occurs through the pores of the solid, with the vapour diffusing out to the surface and the interface temperature starts to increase. At this stage an internal diffusion resistance in the drying material increasingly controls the speed of the drying process. This drying process ends when the solid achieves the equilibrium moisture content with the surrounding medium.

Available models to describe the drying kinetics of thick materials like ceramic tiles can be classified in general models (equilibrium drying model and characteristic drying curve), lumped diffusion models and retreating front models (2). Several models have been developed and applied to the drying of flat, porous materials, based on the diffusion of water content trough the solid (3-8). Recently, models based on the Fick

differential diffusion equation were used to model the drying curves of clay tiles under different experimental conditions (9-12). In these works an effective diffusion coefficient was used to take into account all secondary types of mass transfer. However, they assume that the drying process mainly occurs through the second drying period due to the low moisture content, the moisture transport occurs only by diffusion being the diffusion coefficient constant, and the temperature of the solid immediately reaches the drying temperature having thus a constant value. Therefore, in these models only the isothermal convective drying process is considered. The effect of temperature variation on the ceramic tile drying process has only recently been considered (13-19). These previous works perform simulations of the drying kinetics considering the surface temperature and temperature profiles inside the solid.

Usually drying curves are monotonously decreasing functions with time and it is not too difficult to describe such kind of functions, because many two parameter functions may do well. However, in the case in which an excellent agreement between experiment and model is obtained, it does not really say anything about the correctness of the model (2). It is recommended that for approximate methods, that require a priori information about the type of diffusion relationship, more physical information is inserted.

Conventional isothermal models tend to display two drawbacks: 1) they fail to reproduce correctly the behaviour of the pieces in the first drying stages, and 2) they usually make the initial assumption that the surface moisture content of the piece is in equilibrium with atmosphere at all times. However, this important assumption, though reasonable in principle, has not been verified. The foregoing evidences the need to apply a kinetic model which accounts for the first drying stages (which are the most critical) and considers the evolution of the drying temperature with time.

In this work, a non-isothermal model was developed. The model assumes that two processes take place during the drying of a ceramic tile: diffusion of water content through the pores of the solid material and a water desorption process at the tile surface. Both mechanisms being dependant on the drying conditions (temperature and relative humidity of the drying air) and the tile properties (bulk density of the shaped solid and microstructure).

The present study has been undertaken to optimise the drying stage in ceramic tile manufacture. In this work, 150x150 mm tiles have been shaped and drying tests have been carried out in a pilot-scaled dryer. Initially, the evolution of the tile temperature has been obtained and the inaccuracy of the isothermal model has been stated. Because of this a non-isothermal model was developed and used to model experimental data of drying curves obtained under different experimental conditions of temperature (T =40 ºC – 140 ºC), bulk density of the shaped solid (ρ = 1943 kg/m^3 – 2150 kg/m^3) and tile thickness (s = 8 mm – 10 mm). The dependence of drying kinetics on the internal microstructure of the solid was established.

2 Materials and measurement techniques

2.1 Shaping and characterization of materials

All the tests were conducted with an agglomerated press powder obtained industrially by spray drying an aqueous suspension of ceramic raw materials. The raw materials composition was a standard composition used in the manufacture of red-firing stoneware tiles (hereafter, the stoneware composition). Table 1 shows the mineralogical composition of the spray dried press powder, obtained by X-Ray Diffraction (XRD). The size distribution of the agglomerates was measured by means of laser diffraction with the help of a Mastersizer S (Malvern Instruments Ltd.). Figure 1 shows the results obtained.

Test pieces were formed by uniaxial pressing in a semi-industrial hydraulic press of 120 t of maximum pressing force, Maer 120T (Maer srl) that reproduces the industrial forming process. The pieces measured 150 x150 mm, were of parallelepiped geometry and had different thicknesses and densities. After shaping, the ceramic tiles were stored in sealed plastic bags to maintain their moisture content until the drying test was conducted. The bags were kept under controlled conditions of temperature (T=20ºC) and high relative humidity (φ = 0.9) in order to avoid any possible evaporation of water content. Tiles were weighted before and after the storage to check no changes in the moisture content. Under the experimental conditions of this work, the methodology provided good results and evaporation of water was avoided. However, for higher moisture contents, other methodologies such as the use of metallised packaging could be used as more effective vapour barrier, providing more reliable results.

Press powders were shaped at three different moisture contents, X_0, (5, 6 and 7% kg water/kg dry solid) and three pressing pressures, P, (15, 25 and 40 MPa) providing different thickness, bulk density and microstructure.

After the test pieces were pressed and dried in an oven at 120ºC for 2 h, they were characterised, measuring their bulk density, ρ, and the coefficient of permeability, K_p. Bulk density was measured by the mercury displacement method. In this method the test piece is immersed into a mercury containing receptacle, set on an electronic balance. The upthrust of the immersed specimen is measured directly by the balance. Bulk density is calculated from the expression:

$$\rho=\frac{m_1}{m_2}\rho_{Hg} \quad \textbf{(1)}$$

where m_1 is the mass of the test piece, m_2 is the upthrust registered by the balance and ρ_{Hg} is the density of mercury.

The coefficient of permeability is measured by means of an experimental assembly that measure the pressure loss when air circulates through the piece. The test piece is introduced in the cell and air is forced to flow through the sample. It is registered the time needed for a known volume of air to go through the test piece. The resulting pressure loss at this air flow rate of air is also registered and used to calculate the coefficient of permeability. The following equation has been obtained for porous cylindrical samples form the Darcy's general equation (25) :

$$K_p = \frac{2\mu_a Q_v h}{S} \cdot \frac{P_2}{(P_1^2 - P_2^2)} \quad \textbf{(2)}$$

where μ_a is the air viscosity, Q_v is the air flow rate, h is the sample thickness, S is the air inlet section, P_1 is established as atmospheric pressure and P_2 is defined as $P_2 = P_1 + \Delta P$, where ΔP is the pressure loss.

2.2 Measurement of tile surface moisture content

Tile surface moisture content was measured with a near infrared moisture sensor MM710 (NDC Infrared Engineering) (calibrated for the material studied), logging the moisture data as a function of time with an acquisition rate of 1 Hz. The test was carried out with tiles pressed at the same initial moisture content (6%) and bulk density (2060 kg/m^3). The experimental assembly used is schematically illustrated in Figure 2.

2.3 Drying

Drying tests were carried out in a pilot scale drier so the drying curves were obtained under different experimental conditions. The experimental set-up (Figure 3) is composed of a drying chamber with a grid where the wet tile is placed. The evolution of

the moisture content with time is registered by means of a balance connected to a computer with an acquisition rate of 0.1 Hz. Temperature and humidity sensors are connected to a PID control system acting on the heaters (two electrical heaters of 9 kW), the water nebulizer or the inlet of external air. Type T thermocouples with an accuracy of 0.1ºC and a relative humidity sensor with an accuracy of 2% were used. This configuration allows to establish and to control simultaneously the experimental conditions of temperature and relative humidity of the drying air.

3 Development and calibration of the thermal model

3.1 Analysis and limitations of the isothermal model

The model for drying kinetics of ceramic tiles under isothermal conditions assumes that the drying mechanism is essentially diffusional through the pores of the solid and that the effective diffusion coefficient D is independent of moisture content. The evolution of moisture content (X) with time at any point in the piece may be determined from (20):

$$\frac{\partial X}{\partial t} = D\,\nabla^2 X \qquad \textbf{(3)}$$

To solve the foregoing equation it is necessary to specify the boundary conditions which are obeyed at the top and bottom surfaces of the piece (Σ) . The model assumes that the surface of the piece immediately reaches the drying temperature and the surface moisture content equals the equilibrium moisture with the surrounding air. Thus the boundary conditions adopt the form:

$$T_\Sigma = T_a \qquad \textbf{(4)}$$

$$X_\Sigma = X_e \qquad \textbf{(5)}$$

where T_Σ is the surface temperature, T_a is the drying air temperature, X_Σ is the moisture content at the tile surface and X_e is equilibrium moisture content with the surrounding

air. In addition, temperature in the isothermal model is assumed to be uniform throughout the piece and to remain constant over time.

In order to study the applicability of the isothermal model, a series of laboratory experiments were conducted. To analyse the first boundary condition (Equation 4), tile top (T_T) and bottom (T_B) surface temperature and temperature inside the drying chamber (T_a) were measured. The results are plotted in Figure 4. The figure shows that while the air quickly reaches the set temperature, this is not the case with tile surface temperatures. Therefore, although the gas temperature is constant, drying under these conditions is non-isothermal.

In order to verify the second boundary condition (Equation 5) tile surface moisture content was measured with the experimental assembly depicted in Figure 2 at different air velocities, *v*, (0.5, 2 and 3 m/s) in pieces with the same initial moisture content and bulk density. Ambient conditions were: relative humidity 65% and temperature 298 K. Results obtained are shown in Figure 5. It can be observed that the surface moisture content is not constant and tile surface does not reach equilibrium moisture content at any time, in contrast to the assumption in the second boundary condition. The moisture content decreases continuously as the drying process takes place and the surface temperature increases.

The fact that the drying rate increases when the air velocity is raised from 0.5 to 2 m/s is because the removal of water vapour from the tile surface is favoured by convection (21). However, an additional rise in air velocity from 2 to 3 m/s does not improve further drying, because under these conditions the process is controlled by the migration of water from inside the solid, which is independent of air velocity.

Once the assumed boundary conditions and hypotheses were checked to not be valid, the isothermal model was expected to do not accurately fit the experimental data.

Figure 6 shows an experimental drying curve modelled using the isothermal model. It can be observed that the model do not fit the experimental results. This confirms the need, noted above, for the development of a non-isothermal model that reproduces more accurately the ceramic tile drying process in industrial dryers (developed in next sections but also shown in the figure).

3.2 Development of the non-isothermal model

The model for drying under non-isothermal conditions also assumes that the moisture removal mechanism is essentially diffusional. Therefore, the following equation can be applied:

$$\frac{\partial X}{\partial t} = \nabla \cdot (D \nabla X) \quad \textbf{(6)}$$

This expression allows determining the variation of moisture content in the tile with time. On the other hand, the heat transfer equation in the tile can be written as (22):

$$\rho c_p \frac{\partial T}{\partial t} = k \nabla^2 T + G_E \quad \textbf{(7)}$$

where ρ is the bulk density of the tile, c_p is its specific heat and k is its thermal conductivity. The heat generation term G_E takes into account the variation of thermal energy as a result of water evaporation. If L_V is the enthalpy of vaporisation of water (at the temperature considered), heat generation can be written as:

$$\frac{G_E}{\rho} = L_V \frac{\partial X}{\partial t} \quad \textbf{(8)}$$

Combining all the expressions yields a system of equations in partial derivatives, which adopts the form:

$$\frac{\partial X}{\partial t} = \nabla \cdot (D \nabla X) \quad \textbf{(9)}$$

$$\frac{\partial T}{\partial t} = \nabla \cdot (\beta \nabla X) + \alpha \nabla^2 T \quad \textbf{(10)}$$

where $\beta=L_v D/c_p$ and α is thermal diffusivity: $\alpha=k/(\rho c_p)$

In equations 9 and 10, in a first approximation, thermal conductivity (k), specific heat (c_p) and bulk density (ρ) of the tile may be assumed independent of tile temperature and moisture content. However, the effective diffusion coefficient (D) may vary with temperature and moisture content according to an equation in which more parameters are introduced, similar to Equation (11).

$$D = D_0(1 - bX^n)\exp\left(-\frac{\Theta_D}{T}\right) \quad \textbf{(11)}$$

However, in some preliminary tests a reduced set of temperatures was used (40, 80 and 120 ºC) in order to evaluate this dependence. In Figure 7 evolution of top and bottom temperatures of the samples as well as the moisture content is shown. It can be observed that when the drying temperature and the heating rate is increase, the difference between top and bottom temperatures also increases. Due to the fact that the diffusion coefficient strongly depends on the temperature, this lack of uniformity introduces an uncertainty in the results. To consider the influence of X on D more accurate results are needed, so the setup probably should be changed and a new design of the drying chamber would be needed. In order to do not increase the complexity of the model, the dependence of effective diffusion coefficient on temperature was only considered, which, as studies have shown (7), follows an Arrhenius-type relation:

$$D = D_0\exp\left(-\frac{\Theta_D}{T}\right) \quad \textbf{(12)}$$

where D_0 and Θ_D are constant.

In Figure 7 the drying curves for the preliminary tests modelled considering only the influence of temperature are show. As the model shows a very good agreement with the experimental data it can be concluded that, for the moisture content range of these

ceramic materials, the effective diffusion coefficient depended much more on temperature than on moisture content, and the influence of this variable can be neglected, thus reducing the complexity of the model while providing good results.

To solve energy and mass balances two boundary conditions need to be taken into account. The first one refers to the surface temperature, which varies with time as shown in Figure 4:

$$T = T_{\Sigma} \quad \textbf{(13)}$$

The second boundary condition defines the moisture content in the tile surface at a given moment. As remarked above, the moisture content not only is not equal to equilibrium moisture content but also it varies with time, even under good gas circulation conditions (Figure 5). Therefore, an equation was proposed to take into account this variation of surface moisture content with time:

$$-\frac{dX_{\Sigma}}{dt} = k_X\,(X_{\Sigma} - X_e) \quad \textbf{(14)}$$

Equation 14 means that the rate of variation of surface moisture content (absorbed moisture) is proportional to the difference between the moisture that exists at a given time and the equilibrium moisture content. This process can be related to a water desorption process at the tile surface. Therefore, constant k_X could be interpreted as the kinetic constant of this desorption process and an Arrhenius-type relation was postulated to relate the desorption with temperature:

$$k_X = k_{X,0} \exp\left(-\frac{\Theta_k}{T}\right) \quad \textbf{(15)}$$

where $k_{X,0}$ and Θ_k constant.

Finally, in order to apply the desorption kinetics equation it is necessary to know the evolution of equilibrium moisture content with time. Equilibrium moisture content

depends on the temperature (T) and relative humidity (φ) of the air in contact with the piece. For a given temperature the relation $X_e(\varphi)$ is known as the *equilibrium isotherm*. Although there are many expressions for $X_e = X_e(\varphi,T)$, most of which are empirical or semi-empirical, no valid equation could be found in the entire range of relative humidities and air temperatures analysed, in the literature reviewed. The Henderson isotherm, one of the most widely used isotherms in ceramic materials (23), entails the problem that the parameters on which it depends are not constant over the entire range of relative humidities, making it necessary to use two sets of parameters, for low and high relative humidities, respectively.

From these previous considerations, a very simple empirical polynomial expression was proposed to represent the equilibrium isotherm, $X_e = X_e(\varphi)$. Regarding that for $\varphi = 0$, $X_e = 0$ must be obeyed, the lowest-degree polynomial that fits the experimental data adopted the form:

$$X_e = c_1'\varphi + c_2'\varphi^2 + c_3'\varphi^3 \quad \textbf{(16)}$$

It was empirically established that for a given relative humidity the variation in equilibrium moisture content fitted an exponential equation, which finally allowed the derivation of the expression sought:

$$X_e(\varphi,T) = A_X e^{-\lambda(T-T_R)}\varphi(c_1 + c_2\varphi + \varphi^2) \quad \textbf{(17)}$$

where A_X, λ, c_1 and c_2 are empirical constants and T_R is the reference temperature (T_R =273 K).

4 Calibration of the non-isothermal model under laboratory conditions

In order to apply the developed model, the equilibrium isotherms as well as the parameters $k_{X,0}$, Θ_k, D_0 and Θ_D need to be previously known. In addition, it was necessary to analyse the influence of the drying cycle and the characteristics of the tile

on the parameters of the model. The system of differential equations (Equation 9 and 10) was solved using the implicit finite differences method (24) with the help of a resolution algorithm programmed in C++.

4.1 Equilibrium isotherm

The equilibrium moisture content of the spray-dried stoneware powder was determined in a Heraeus Votsch HC 2020 climatic chamber. Tests were carried out at three different temperatures (40ºC, 60ºC and 80ºC) and three relative humidities of the air (0.25, 0.5 and 0.9).

Figure 8 shows the experimental results obtained together with the fitting of the data to Equation 17. For the studied material, the parameters in the equation were as follows: A_X = 0.3291 kg water/kg dry solid; λ = 0.0311 K^{-1}; c_1 = 0.680; c_2 = -1.226. This correlation was used to determine the equilibrium moisture content between de ceramic tile and the drying air under the different experimental conditions tested.

4.2 Desorption kinetics

As has been established before the drying kinetics comprises two steps: water migration from inside the piece to the surface and desorption from the surface. The former depends on the thickness of the piece, whereas the latter does not. Therefore, one way of isolate both processes in order to study the desorption kinetics is to conduct drying tests either with very thin pieces or with a layer of unshaped spray-dried powder. In this work, the second option was chosen to determine the desorption coefficients.

In order to do that, quasi-isothermal tests were conducted (constant temperature in the drying chamber but not in the solid surface). The material (spray-dried stoneware powder) was spread on a tray set in the dryer chamber. The evolution of the moisture

content and the solid temperature during the drying process was registered by means of the balance connected and a J-type thermocouple held to the sample. The test powders had an initial moisture content of 6% and three drying cycles with different maximum temperatures (40 ºC, 60 ºC and 80ºC) were selected.

Figure 9 shows the experimental drying curves for the spray-dried powders. Data were fitted to Equation 14 and the desorption constant was obtained at different temperatures. Finally, from Equation 15 the following values for the desorption parameters were obtained: $k_{X,0}$ = 100 s^{-1} and Θ_k = 3150 K.

The correlation resulting for the material tested can be used to model the desorption process that takes place at the tile surface during the drying process, under different experimental conditions of air temperature.

4.3 Drying kinetics

Influence of the drying temperature

Ceramic tiles were dried under different experimental conditions of drying temperature in order to study its influence on the drying kinetics and the parameters of the model proposed. In order to reproduce industrial drying, in which temperature does not remain constant throughout the entire cycle, the pieces were heated from ambient temperature to the maximum drying temperature (40, 60, 80, 100, 120 and 140ºC) at a constant heating rate. The purpose was to reproduce the drying curves at different temperatures, with the same set of parameters. If this was possible, the model would probably be applicable to curves for arbitrary temperatures and, in particular, to the temperature curve of an industrial dryer.

Tests were conducted in the pilot-scale dryer on test pieces pressed at 6% of moisture content and a pressing pressure of 25 MPa. Under these conditions the

thickness of the shaped body and its bulk density were kept constant and equal to 8 mm and 2060 kg/m^3, respectively.

Figure 10 shows the drying curves obtained for the six temperatures analysed. Experimental data were modelled using Equations 9 and 10, and the boundary conditions established (Equations 13 and 14). From the fitting of the data, parameters in the diffusion equation were found and the following values were obtained: $D_0 = 2.6 \cdot 10^{-4}$ m^2/s; $\Theta_D = 3800$ K.

It can be observed that theoretical and experimental drying curves show a good agreement. This means that parameters obtained for the desorption constant and the diffusion coefficient can be introduced in the model proposed to simulate the drying process of ceramic tiles dried at different temperature conditions, thus validating the model. It can be observed some deviations of the model for high temperatures, that could be avoid if non constant parameters were used. However, the difficulty of the simulation would be increases. In this work a commitment between accuracy and resolution difficulty has been achieved and the non-isothermal model, with constant parameters, can be used to simulate the drying process accurately enough.

Influence of bulk density and tile thickness

The foregoing tests were focused on confirming the applicability of the kinetic model at different maximum drying temperatures, without varying any characteristic of the tiles. However, in industrial application, tile density and thickness may change; this made it of interest to establish how the parameters of the drying model vary with these changes.

In order to analyse the influence of the bulk density, ρ, on the drying kinetics, drying tests were conducted with pieces made of the same material (spray-dried stoneware powder) shaped at different moisture contents (5, 6 and 7% kg water/kg dry

solid) and pressing pressures (15, 25 and 40 MPa), which yielded a wide range of bulk densities (Table 2). The tile thickness (8 mm) and the drying temperature curve (120ºC) were kept constant in every test.

In Figure 11 the drying curves obtained are shown. Experimental data were modelled and the applicability of the model and the parameters previously obtained was verified. It was found that parameters $k_{X,0}$, Θ_k and Θ_D did not change with bulk density and their values were constant ($k_{X,0}$ = 100 s^{-1}; Θ_k = 3150 K; Θ_D = 3800 K).

The fact that $k_{X,0}$ and Θ_k remained constant was reasonable since they are related to the desorption process; this occurs at the surface and must be independent, therefore, of bulk density. The experimental results obtained corroborate that desorption kinetics only depends on the sort of material and particle size distribution (specific surface area), but not on the bulk density of the material, since the use of the same desorption parameters allows the kinetic model to be fitted for pieces with different density.

However, the bulk density influences the internal microstructure and porosity of the tile and the diffusion of water through it. Therefore, only the diffusion coefficient is modified. In this case, the pre-exponential factor, D_0, is the parameter that depends on the bulk density. Table 2 shows the values obtained for each experimental condition tested.

The influence of the tile thickness was analysed by performing tests with pieces of two different thicknesses: 8 and 10 mm. The test pieces were shaped at a powder moisture content of 6% and pressing pressure of 25 MPa and were dried in the at a maximum drying temperature of 130ºC.

The drying curves are shown in Figure 12. Experimental data were modelled using the non-isothermal model proposed showing a good agreement. The different parameters of the model that are intrinsic characteristics of the material ($k_{X,0}$, Θ_k and

Θ_D) and do not depend on the geometry of the piece, were the same found for the previous test. However, when the tile thickness is modified but keeping constant the shaping conditions (moisture content and pressing pressure) the bulk density changes and the diffusion coefficient is modified as mentioned before.

From these results it can be concluded that drying curves obtained under different experimental conditions of maximum temperature, bulk density and tile thickness can be modelled using the non-isothermal model proposed. In all cases the model present a good fit, being achieved the maximum deviation between experimental a theoretical values at the early stages of drying, with relative errors lower than 10% in all of them.

5 Relation between microstructure and drying kinetics

From the modelling of the drying curves it was concluded that the only variable that depends on the internal microstructure of the ceramic tile and must be known in order to simulate the drying curves, was the diffusion coefficient. Parameter D_0 is the only one that depends on tile bulk density (ρ) as shown in Table 2. Therefore, it is of interest to obtain a correlation between both variables that can be introduced in the drying model. In Figure 13 the logarithm of D_0 is plotted versus the logarithm of the bulk density and a linear relation was found:

$$\ln D_0 = a_D + b_D \ln \rho \quad \textbf{(18)}$$

On the other hand, the permeability coefficient, K_p, (obtained experimentally for pieces with the same characteristics) also depends on bulk density and is a parameter that can be used to characterize the internal microstructure of a ceramic tile. In Figure 13 it can be observed that the relation between both variables is also linear:

$$\ln K_p = a_K + b_K \ln \rho \quad \textbf{(19)}$$

A direct relation between the diffusion coefficient and tile microstructure (characterised by the permeability coefficient) is thus established. The two preceding expressions then yield an interesting expression which relates the characteristic drying parameter, D_0, to a property (K_p) that quantifies the resistance to gas flow of a porous material:

$$D_0 = aK_p^b \quad \textbf{(20)}$$

where constants a and b adopt the values 0.57 and 0.25, respectively, when D_0 is expressed in m^2/s and K_p is expressed in m^2.

6 Conclusions

In this work the drying kinetics of ceramic tiles was studied. Results showed that the surface temperature of the piece does not reach immediately the drying temperature, being the process non-isothermal. Besides, the surface moisture content also varies with time and does not reach the equilibrium moisture content quickly.

A non-isothermal model was proposed to simulate drying curves under different experimental conditions. The model assumes that two processes take place during the drying of a ceramic tile: diffusion of water content through the pores of the solid material and a water desorption process at the tile surface.

The desorption parameters were obtained from drying curves of a thin layer of spray-dried powder and were checked to be constant and independent on the drying conditions and the tile internal microstructure. The only variable depending on the bulk density of the shaped material was the parameter D_0 in the coefficient diffusion equation. A correlation was found so it could be introduced in the model which was validated showing good agreement with the experimental results.

Finally, a relationship between D_0 and the tile permeability (K_p) was established. This relation is especially interesting since it establishes a link between the ease of drying and the resistance to gas flow of a porous material.

References

[1] Mujumdar, A.S. Handbook of Industrial Drying; Taylor and Francis, 2006.

[2] Coumans, W.J. Models for drying kinetics based on drying curves of slabs. Chemical Engineering and Processing 2000, 39, 53-68.

[3] Scherer, G.W. Theory of drying. Journal of the American Ceramic Society 1990, 73, 3-14.

[4] Tomas, S.; Skansi, D.; Sokele, M. Convection drying of porous material. Ceramics International 1994, 20, 9-16.

[5] Derdour, L.; Desmorieux, H. An analytical model for internal moisture content during the decreasing drying rate period. AIChE Journal 2008, 54, 475-486.

[6] Chai, A.; Vakhguelt, A. Simulation on effects of porosity pattern arrangement of porous media during drying. AIP Conference Proceedings 2012, 1440, 356-360.

[7] Escardino, A.; Gallego, M.A.; Felíu, C.; Barba, A.; Sánchez, E. Drying of ceramic materials shaped by unidirectional pressing: I kinetic model. British Ceramic Transactions 1993, 92 (5), 197-202.

[8] Sander, A.; Skansi, D.; Bolf, N. Heat and mass transfer models in convection drying of clay slabs. Ceramics International 2003, 29 , 641-653.

[9] Vasic, M.; Radojevic, Z.; Grbavcic, Z. Calculation of the effective diffusion coefficient during the drying of clay samples. Journal of the Serbian Chemical Society 2012, 77 (4), 523-533.

[10] Vasic, M.; Grbavcic, Z.; Radojevic, Z. Analysis of moisture transfer during the drying of clay tiles with particular reference to an estimation of the time-dependent effective diffusivity. Drying Technology 2014, 32, 829-840.

[11] Vasic, M.; Grbavcic, Z.; Radojevic, Z. Determination of the moisture diffusivity coefficient and mathematical modelling of drying. Chemical Engineering and Processing: Process Intensification 2014, 76, 33-44.

[12] Vasic, M.; Radojevic, Z. Drying simulation of shrinkable clay tiles using variable diffusivity model. Advanced Materials Research 2014, 837, 506-510.

[13] Pang, S.; Haslett, A.N. High-temperature kiln drying of softwood timber. The role of mathematical modelling. In Mathematical modelling and numerical techniques in drying technology, ed. I. Turner & A.S. Mujumbar. Marcel Dekker, New York, 1997, 179-220.

[14] Chemkhi, S.; Zagrouba, F.; Bellagi, A. Drying of ceramics: modelling of the thermo-hydro elastic behaviour and experiments. Industrial Ceramics 2005, 25 (3), 149-156.

[15] Keum, YT.; Auh, KH. An efficient numerical method for incorporating phase changes in ceramic drying process. Journal of Ceramic Processing Research 2002, 3 (3), 141-145.

[16] Mallol, G.; Cantavella, V.; Feliu, C.; Llorens, D. Study of ceramic tile drying under non-isothermal conditions and its industrial application. Key Engineering Materials 2001, 213, 1755-1758.

[17] Belhamri, A. Characerization of the first falling rate period during drying of a porous material. Drying Technology 21, 1235-1252, 2003.

[18] Chai, A.; Rigit, A.; Ung, H.H. Heat transfer and computational simulations on the drying process of a kiln. Proceedings of the ASME Summer Heat Transfer Conference 2005, 2, 583-588.

[19] Shokouhmand, H.; Hosseini, S.; Abdollahi, V. Numerical simulation of drying a porous material using the lattice Boltzmann method. Journal of Porous Media 2012, 15, 303-315.

[20] Mujumdar, A.S. (Ed.). Advances in drying. Hemisphere: Washington, 1980.

[21] Barba, A.; Escardino, A.; Moreno, A.; Negre, F. Secado de soportes cerámicos para pavimento de monococción. In XXX Congreso nacional de cerámica y vidrio. 1990.

[22] Incropera, F.P.; Lavine, A.S; DeWitt, D.P. Fundamentals of heat and mass transfer. 3rd ed. John Wiley & Sons: New York, 1990.

[23] Escardino, A.; Jarque, J.C.; Moreno, A.; Torre, J. Secado de materiales cerámicos (I) consideraciones generales. Isotermas de equilibrio. Técnica Cerámica 1990, 185, 452-462.

[24] Celia, M.A.; Gray, W.G. Numerical methods for differential equations: fundamental concepts for scientific and engineering applications. Prentice-Hall: Englewood Cliffs, 1991.

[25] Amoros, J.L.; Beltran, V.; Escardino, A.; Orts, M.J. Air permeability of fired ceramic floor tile bodies. I. Influence of pressing variables and burning temperature. Boletin de la Sociedad Española de Ceramica y Vidrio 1992, 31, 33-38.

Figure captions

Figure 1. Grain size distribution of the spray dried press powder.

Figure 2. Scheme of the experimental assembly used to measure surface moisture content (X_S).

Figure 3. Pilot scale dryer set-up.

Figure 4. Comparison of drying chamber temperature and tile surface temperature.

Figure 5. Variation of tile surface moisture content with air velocity.

Figure 6. Fit of the experimental data to the isothermal and the non-isothermal model.

Figure 7. Moisture and temperature evolution as a function of time for checking of influence of parameter on the diffusion coefficient.

Figure 8. Equilibrium isotherms.

Figure 9. Drying curves of spray dried powder. Modelling of the desorption process.

Figure 10. Influence of maximum drying temperature.

Figure 11. Influence of bulk density.

Figure 12. Influence of tile thickness.

Figure 13. Influence of bulk density on D_0 and K_p.

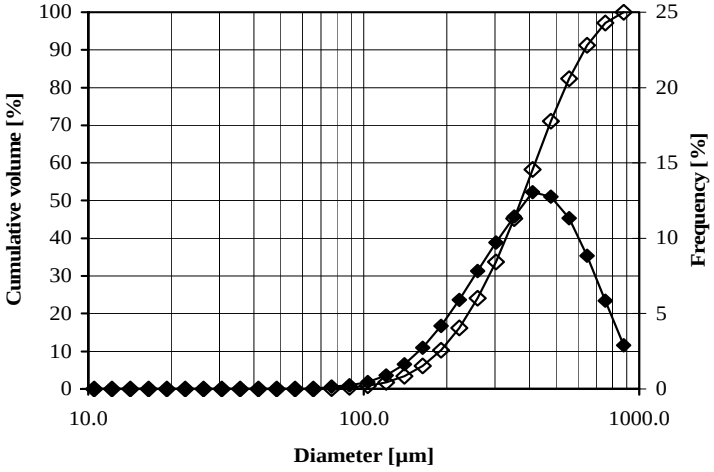

Figure 1. Grain size distribution of the spray dried press powder.

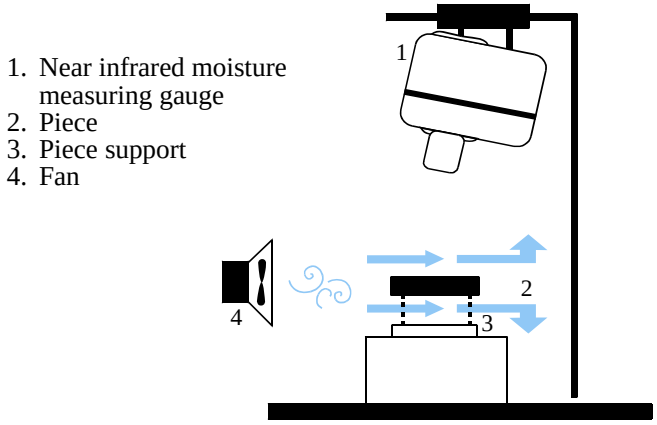

Figure 2. Scheme of the experimental assembly used to measure surface moisture content (X_{Σ}).

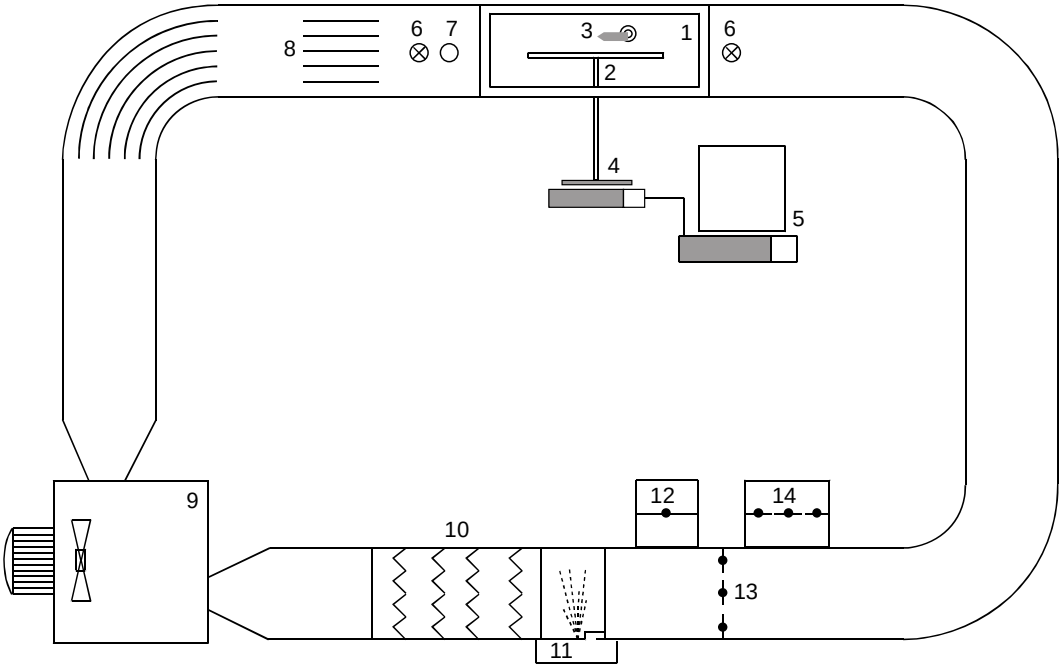

1. Drying chamber
2. Grid
3. Pitot tube
4. Balance
5. Data acquisition
6. Temperature sensor
7. Humidity sensor
8. Flow guides
9. Fan
10. Electric heaters
11. Water nebulizer
12. External air inlet
13. Recirculation valve
14. Purge valve

Figure 3. Pilot scale dryer set-up.

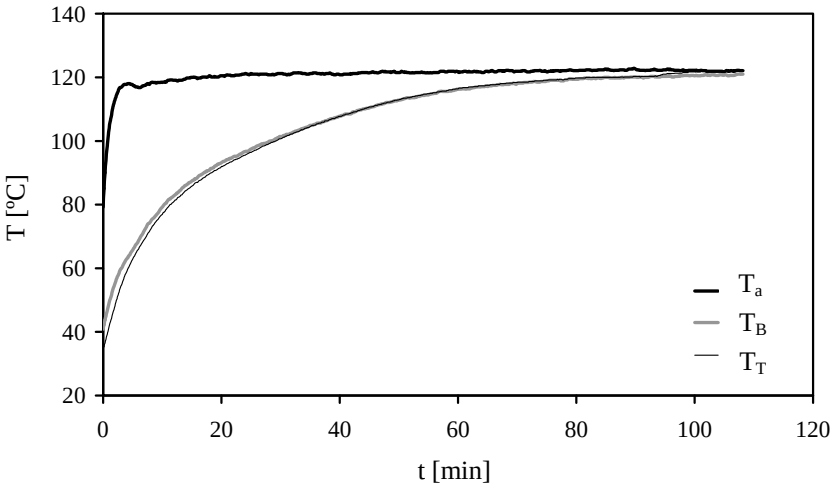

Figure 4. Comparison of drying chamber temperature and tile surface temperature.

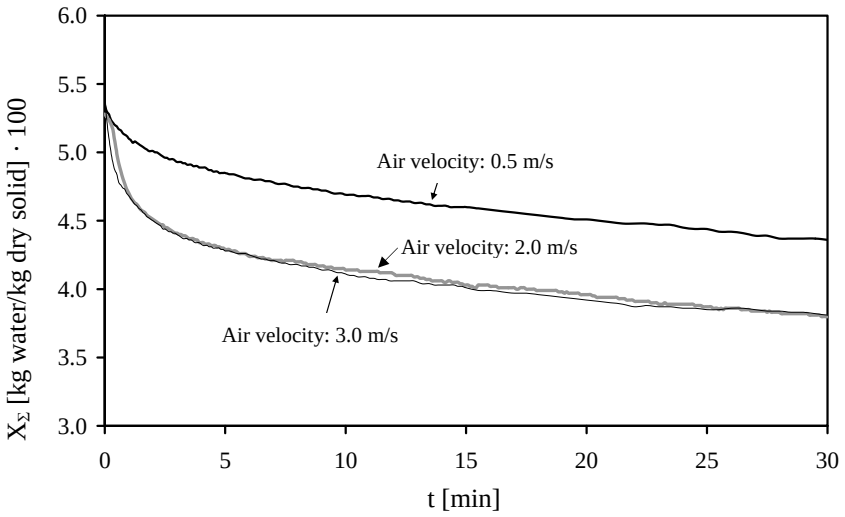

Figure 5. Variation of tile surface moisture content with air velocity.

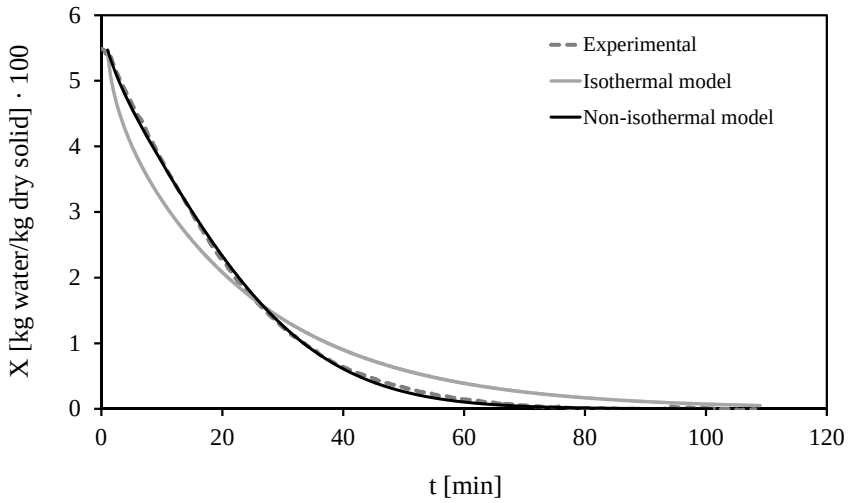

Figure 6. Fit of the experimental data to the isothermal and the non-isothermal model.

.

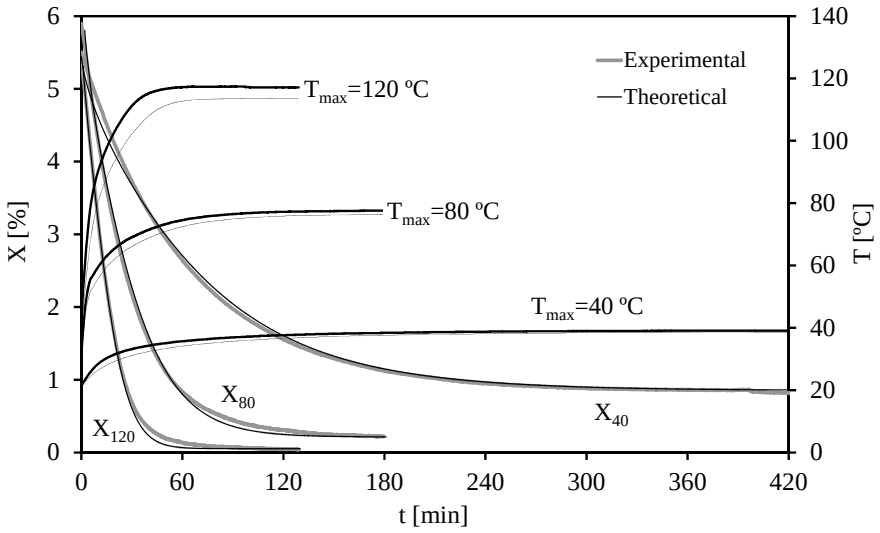

Figure 7. Moisture and temperature evolution as a function of time for checking of influence of parameter on the diffusion coefficient.

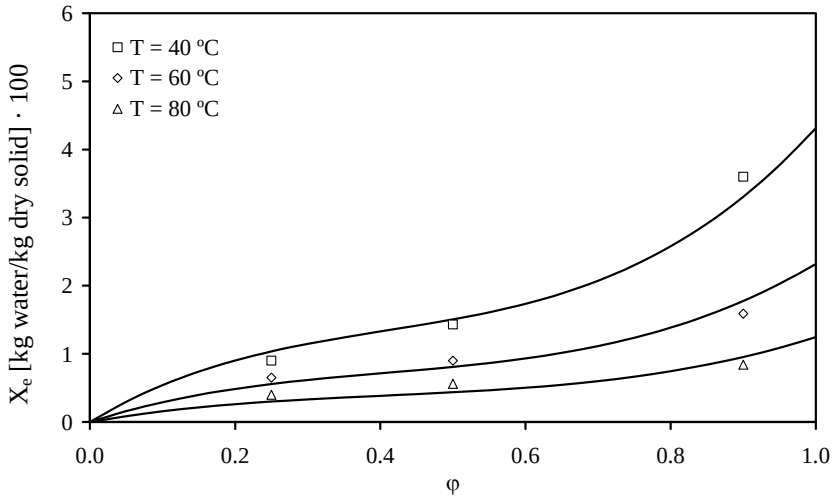

Figure 8. Equilibrium isotherms.

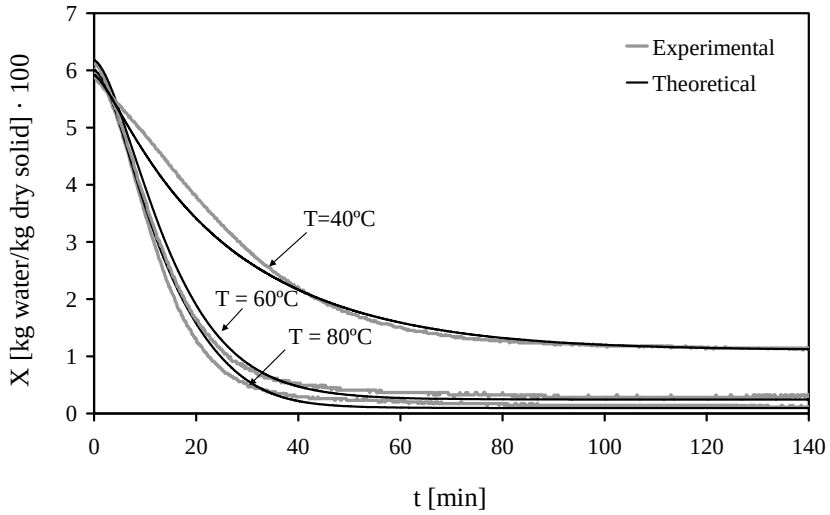

Figure 9. Drying curves of spray dried powder. Modelling of the desorption process.

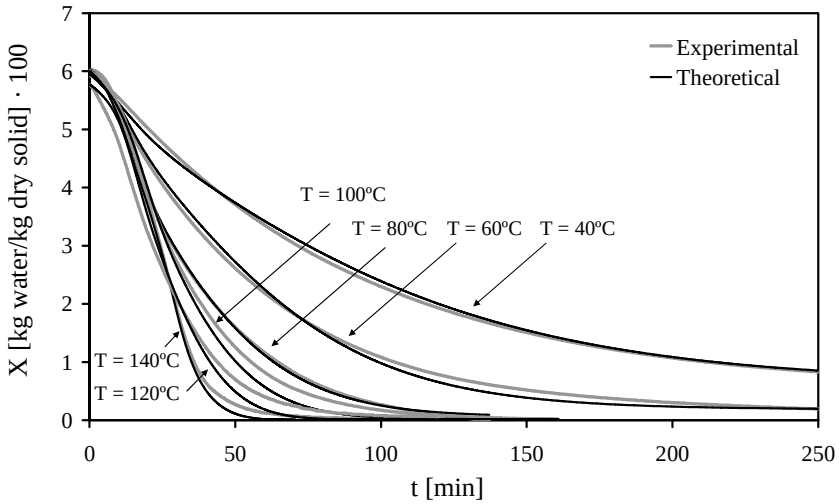

Figure10. Influence of maximum drying temperature.

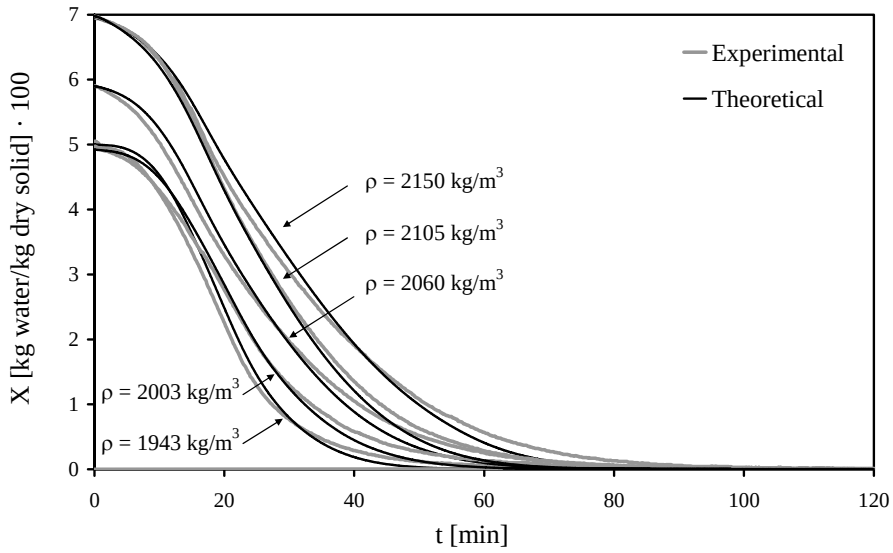

Figure 11. Influence of bulk density.

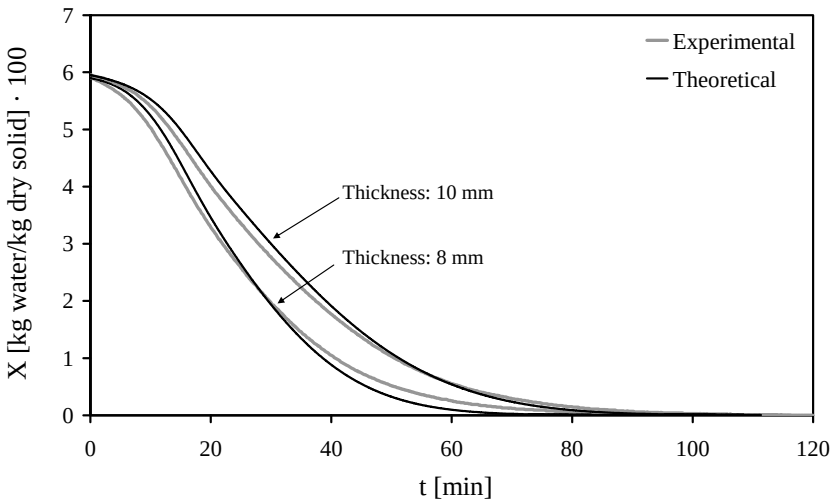

Figure 12. Influence of tile thickness.

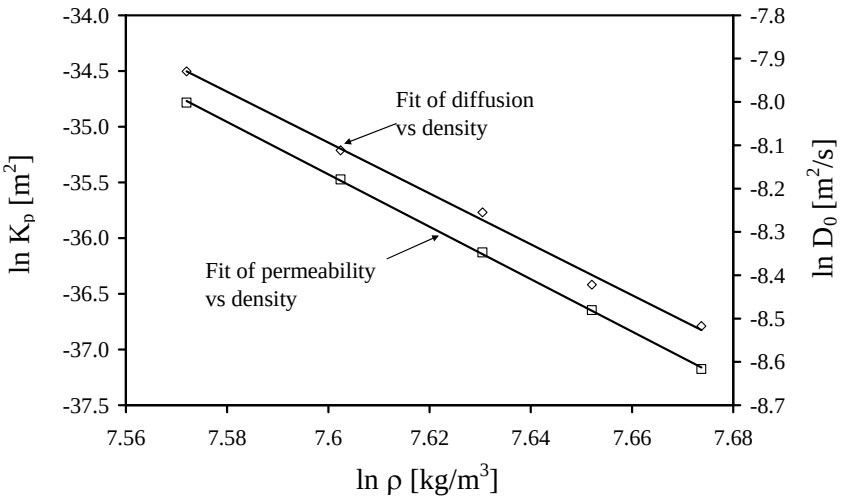

Figure 13. Influence of bulk density on D_0 and K_p.

Table captions

Table 1. Mineralogical composition of the spray dried press powder

Table 2. Bulk density and parameter D_0 at different pressing pressure and moisture content.

Table 1. Mineralogical composition of the spray dried press powder

Mineral	Mass load [%]
Quartz	36 - 39
Kaolinite	17 - 21
Chlorite	2 - 4
Carbonates	4 - 5
Illite	14 - 19
Sodium Feldspar	10 - 14
Hematite and other compounds	7

Table 2. Bulk density and parameter D_0 at different pressing pressure and moisture content

P [MPa]	X_0 [kg water/ kg dry solid]· 100	ρ [kg/m^3]	D_0[m^2/s]·10^4
15	5	1943	3.6
15	7	2105	2.2
25	6	2060	2.6
40	5	2003	3.0
40	7	2150	2.0